Application of a "Spraylet" Model to the Simulation of Fuel Spray Autoignition

Ch. Eigenbrod*, K. Klinkov, M. Reimert, P. Rickmers
Center of Applied Space Technology and Microgravity (ZARM), University of Bremen, Germany
christian.eigenbrod@zarm.uni-bremen.de

Abstract

The numerical simulation of spray autoignition is a challenging task. The instant of ignition at given ambient conditions regarding temperature, pressure and turbulence of flow depends on droplet sizes, droplet dispersion, droplet vaporization and mixture formation and residence time. The core element of a spray is the droplet and its surrounding but interactions between neighboring droplets and between droplets and the partially premixed surrounding plays an important role. The presented "Spraylet" simulation deals with all this in a split way. The first task, the dispersion of droplets into a turbulent flow as well as the vaporization and mixture formation is simulated applying a commercial CFD-code. From this vaporizing two-phase flow the droplet trajectories and the gas phase parameters along these trajectories are extracted to serve as variable boundary conditions for the second task, the one dimensional single droplet ignition simulations, which are fully transient and based on comprehensive chemistry. These droplet simulations are named "Spraylet" as the approach shows similarities to laminar "Flamelet"- simulations dealing with chemistry in a turbulent reacting single phase flow. The obtained ignition delay times can be transformed into spatial distributions of ignition probability. The droplet simulations using n-heptane are based on single droplet experiments in microgravity and the spray ignition simulations are validated along hot wind-tunnel experiments.

Introduction

Spray combustion systems operating in the lean, prevaporized and premixed regime promise the lowest possible emissions of nitric oxides.

In order to support the development of such an engine that can be safely operated at all conditions, detailed knowledge about the self-ignition process of fuel sprays in hot ambiance is required. Moreover the aim is to numerically simulate spray ignition in premixing inlet ducts of arbitrary configurations.

The computing of a spray ignition process must include a number of numerical models in order to carefully describe all transfer phenomena and chemical reactions occurring in a two-phase flow. The modeling of spray formation needs a multidimensional CFD solver implementing such models as spray atomization, liquid evaporation, turbulent gas-liquid flow field and processes of multi-component oxidation. These models must also take small scale phenomena in the spray into account: the interference of neighboring droplets and non-uniform mixing of a fuel vapor with the gas which surrounds the evaporating droplet. The fact of inhomogeneity seems to be of particular importance for a correct simulation of ignition processes. Additionally, detailed chemical kinetic mechanisms are required for an accurate modeling of spray ignition.

Up-to-date computing technologies have insufficient performance for such detailed simulations. Therefore models with significant simplifications are applied [1-7].

First, dynamic and thermal effects of droplets in a two phase flow are usually considered through averaged properties of mass, momentum and energy. When modeling mixing of fuel vapor with the surrounding gas, the differences between diffusion rates of components as well as the finite penetration of the diffusion fluxes are not taken into account. Last seen in the fact that fuel vapor is uniformly mixed with the gas filling within the calculation cell, whose dimensions are several orders of magnitude larger than the droplet. As a consequence, the chemical reactions in the two-phase medium are represented by volume processes in the computational cell.

Second, there is no complete mechanism available to describe the oxidation process of multi-component real-fuels, so that surrogate fuels are applied. For the reason of limited computing performance in a fully multidimensional CFD simulation, a further reduced chemistry is applied. [7, 8]

Several studies from recent years regard phenomena of single droplet ignition and combustion in an unconfined or finite gas volume [9-14]. Geometrical simplicity of numerical domains for such objects enables to accurately study small scale phenomena in an inhomogeneous gas-vapor mixture surrounding the droplet. Furthermore such models enable to apply detailed chemical kinetic mechanisms, for example, those for multi-component fuels, which are expected in future.

* Corresponding author: Christian.Eigenbrod@zarm.uni-bremen.de

A connection of the large scale 3-D atomization and flow simulation with small scale 1-D droplet modeling opens a way to extend the knowledge of complex interphase phenomena in the framework of spray ignition [15]. The numerical model of such an approach is proposed in the present work. These simulations that were performed over a wide range of parameters are validated by comparison to spray ignition experiments for the first time.

Experimental Facility

The validating experiments were performed in the Bremen hot wind-tunnel (HWT) described in detail in [16]. The hot wind tunnel is a Ludwieg-tube blowdown windtunnel (Figure 1). It consists of a 40 m long charging tube that is filled with air, pressurized and electrically heated by means of resistors. Downstream the charging tube there is a thermally insulating slide valve. This valve shall keep the injection- and measurement section at RT during the lasting heating process of the charging section. This slide valve is opened immediately before each experiment. Further downstream is the injector section injecting the fuel in a jet-in-crossflow (JIC) configuration for this study. The injection section is followed by the measurement section that is equipped with windows, cameras, pressure sensors and photomultipliers to monitor the ignition process. The wind-tunnel ends in a quick-shut valve allowing for opening and closure of the 0.3 m (diam.) tube within 5 ms. This valve also contains an exchangeable nozzle to adjust the flow velocity to the wanted value. When charging of the tube is finished, first the slide valve is opened followed by quickly opening the quick-shut valve. Now the pressurized air can leave the tube through the nozzle. The pressure in the tube drops first at the valve and an expansion wave travels along the tube with the velocity of sound and is reflected at the right end of the tube. From the moment on, the expansion wave arrives at the hot section of the tube, downstream of the wave there is a flow of constant velocity, temperature and pressure. Temperature and pressure are according to the charging parameters minus the pressure (and temperature) drop through the wave. These conditions remain constant until the expansion wave again reaches the injection point. During this period, fuel of a pre-defined amount is injected through a defined nozzle with a pre-defined pressure and the ignition process is observed in the measurement section. The maximum experiment time is according to the length of the tube and temperature in the tube. This is 100 ms and by far long enough as compared to induction times at the relevant temperature conditions. The quick-shut valve is closed prior to the reflected expansion wave arriving at the injection section.

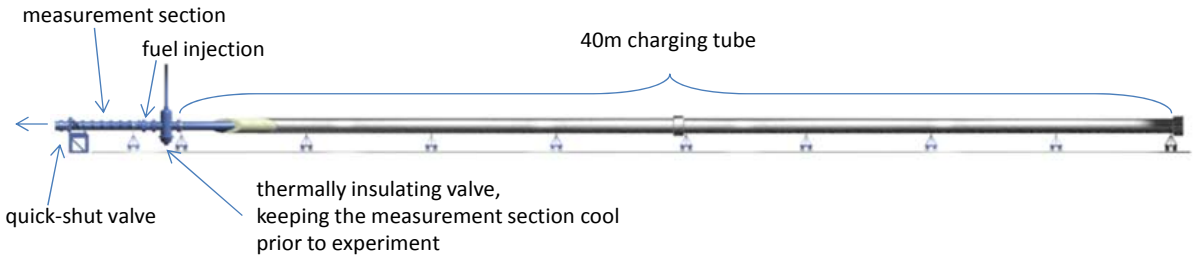

Figure 1 Hot blowdown windtunnel

Nomenclature

t	time
r	radius in spherical coordinates
r_s	coordinate of liquid-gas boundary (droplet radius)
$r_{\max}$	coordinate of outer boundary (domain radius)
p	pressure
T	temperature
ρ	density
m	mass
Z	compressibility factor
$\mathbf{u}$	velocity
$\mathbf{u}_{Di}$	diffusion velocity of species i
c_{pi}	heat capacity of species i
μ_i	molecular weight of species i
$\overline{\mu} = \sum \mu_i X_i$	molecular weight of mixture
X_i	mole fraction of species i
Y_i	mass fraction of species i
λ	thermal conductivity
h_i	specific enthalpy of species i
$h = \sum h_i Y_i$	enthalpy of mixture
$\dot{w}_i$	rate of production of species i by chemical reactions (mass per volume per time)
A_k, n_k, E_k	coefficients of production-rate of k-reaction
$\nu'_{i,k}, \nu''_{i,k}$	stoichiometric coefficients of species i by chemical reaction k as a reagent and as a product
f	fugacity
ϕ	fugacity coefficient
ΔH_v	enthalpy of vaporization

R^0 universal gas constant

$R_i = \frac{R^0}{\mu_i}$ gas constant of species i

φ fuel-air ratio of mixture

Computational Model

As stated above the spray ignition simulation is split into two parts: the large scale flow simulation and the computing of ignition of single droplets of this flow.

The spray simulation involves modeling of a two-phase flow in a domain representing the experiment section of HWT. It considers the following tasks: initial formation of an atomized spray consisting of fuel droplets, evaporation of droplets, turbulent liquid-gas flow field in a large scale grid with a cell size several orders of magnitude larger than a droplet. Chemistry is not taken into account. Droplets trajectories statistically representing the whole spray will be extracted from this evaluation of the spray. Determined parameters consist of initial droplet diameter and local parameters of the gas flow field along the droplet trajectory: the pressure, the relative droplet velocity, the gas temperature and the fuel-air ratio of the mixture. These parameters of selected droplets contain initial and boundary conditions for the spraylet computation – the second part of the spray ignition simulation.

The spraylet simulation considers an ignition process of a single droplet in a domain with variable boundary conditions. Initial parameters and boundary conditions are chosen in such a way that the spray effects of neighboring droplets in the flow are approximated. As the droplet is involved into the heat transfer and evaporation processes, computing of the gas phase includes the heat and mass transfer and chemical reactions which generate numbers of species and release the heat. Achieving the gas temperature of 1300 K is taken as measure to indicate hot ignition.

After processing the spraylet simulations for all selected droplets one gains a distribution of ignition times. Together with the droplet track data it is easy to convert ignition times into ignition points. This gives a required spatial distribution of ignition points in the spray.

Large Scale Spray Simulation

The commercial CFD software ANSYS FLUENT was used as a solver of the large scale numerical problem. The two-phase flow field is calculated using a discrete droplet method (DDM) approach [17]. The gas phase is solved by an Eulerian method, where the equations are considered to be continuous in space and time. The turbulence is described by a realizable k-ε model. Same time, in DDM the liquid phase is represented by droplet parcels. Each parcel contains a large number of droplets that have the same properties. The trajectories of each parcel are calculated using a Lagrangian method.

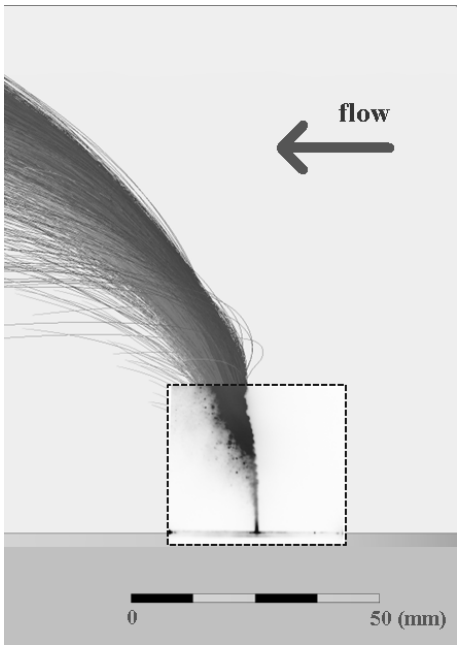

Figure 2 Jet in cross flow injection. Comparison between simulation and experiment

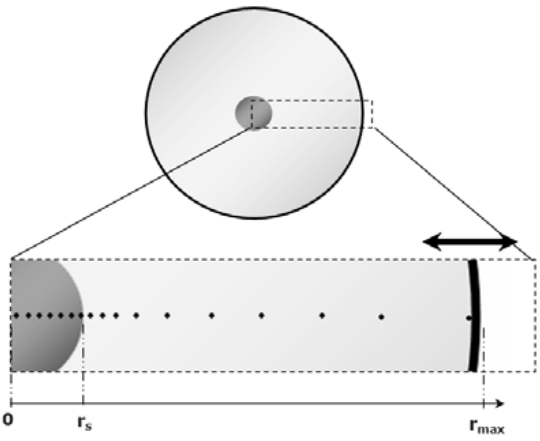

Figure 3 Schematic of the numerical grid and the boundaries of the spraylet model

The discrete phase is also described by sub-models of initial spray atomization, breakup and dispersion. The initial atomization is calculated using a two-parameter Rosin-Rammler distribution model, which takes the nozzle geometry, fluid properties and the flow rate into account. A Kelvin-Helmholtz/Rayleigh-Taylor (KH-RT) model describes the secondary breakup of droplets. The turbulent dispersion model uses a stochastic method including a two-way turbulent coupling between the continuous and the discrete phases. Neither droplet collisions nor coalescence are taken into account. The droplet evaporation is provided by a sub-model for heat and mass transfer.

A numerical mesh of the experiment section of HWT was generated using the software package ANSYS ICEM CFD and includes approx. 2.400.000 tetragonal cells each of them of a volume spanning from approx. 1 to 100 mm^3. The mesh is refined at the location of the spray injection with a length factor of 0.5 mm.

In Figure 2 results of a calculation of the spray injected into the cross flow are shown. The droplet trajectories are overlaid by an experimental photo (dashed line frame) of the spray in the HWT. The incident flow of air with a temperature of 800 K and pressure of 5 bar has a velocity of 25 m/s. The liquid droplets of n-heptane injected with a velocity approx.75 m/s have a temperature of 300 K and sizes within a range from 10 up to 200 µm. Even though the spray characteristics could not be measured, the agreement between simulated and measured JIC-geometries gives rise to the assumption that the real spray pattern are quite well represented through the simulation.

Spraylet Model

Locally, a spray could be represented by a combination of small monodisperse clouds. Formation of the cloud occurs at the moment of a breakdown of a jet core and big droplets under the influence of a gas flow. The clouds move in the flow field not interfering with each other. Under the influence of a gas flow and other clouds the volume of a cloud changes as well as the temperature of the gas within. Trajectories could be calculated beyond the lifetime of the droplets. In such case a fuel vapor representing "cloud of droplets" moves along streamlines.

Droplets in the cloud have equal size and are at equal distance from each other. For the reason of symmetry, a spherical calculation domain can be allocated with a single droplet at the center. There are no vapor and energy fluxes through the boundary of this domain. Changes in the fuel concentration in the cloud result in corresponding changes of the domain diameter. When the droplet evaporates, the diameter changes, but the mass of fuel in the domain remains constant. The spherical symmetry allows for a reduction of the problem to a one-dimensional model. The model is subjected to the following assumptions:

1) no convective flow in the domain;
2) non-equilibrium effects are negligible;
3) no thermal diffusion and radiative heat transfer;
4) no invasion of gas into the liquid phase;
5) surface tension is neglected as its influence is assumed to be minor for higher pressure;
6) no chemical reactions in the droplet.

The numerical model is based on the transient differential energy and matter conservation equations in the liquid and gas phases with variable physical properties [18, 19]. For the liquid phase located in $0 < r < r_s$, where r_s is the droplet radius, we can write:

mass conservation
$$\frac{\partial \rho}{\partial t} + div(\rho \cdot \mathbf{u}) = 0 \tag{1}$$

energy conservation
$$\rho c_p \left(\frac{\partial T}{\partial t} + \mathbf{u} \cdot \nabla T \right) = div(\lambda \nabla T) + \frac{\partial p}{\partial t} \tag{2}$$

equation of state
$$p = \rho Z \frac{R^0}{\mu} T \tag{3}$$

where the compressibility factor $Z(p,T)$, the heat capacity $c_p(T)$ and the thermal conductivity $\lambda(p,T)$ are functions of pressure p and temperature T and calculated by the methods offered in [20]. The droplet radius $r_s(t)$ varies as a result of the liquid evaporation and thermal extension.

The gas phase located in $r_s < r < r_{max}$ consist of a multi-component mixture of fuel vapor, air (nitrogen and oxygen) and reactants of chemical processes from fuel-oxidation. The differential equations for the gas phase include terms of diffusion of species and of chemical production/eduction of species and energy:

mass conservation
$$\frac{\partial \rho}{\partial t} + div(\rho \cdot \mathbf{u}) = 0 \tag{4}$$

components conservation
$$\rho \frac{\partial Y_i}{\partial t} + \rho \mathbf{u} \cdot \nabla Y_i + div(\rho Y_i \cdot \mathbf{u}_{Di}) = \dot{w}_i \tag{5}$$

energy conservation
$$\rho \sum c_{p_i} Y_i \left[\frac{\partial T}{\partial t} + \mathbf{u} \cdot \nabla T \right] - \frac{\partial p}{\partial t} + \sum h_i \dot{w}_i + div(-\lambda \nabla T) + $$
$$+ \rho \sum c_{p_i} Y_i \mathbf{u}_{Di} \cdot \nabla T = 0 \tag{6}$$

equation of state
$$p = \rho \frac{R^0}{\bar{\mu}} T \tag{7}$$

Processes of combustion are characterized by an intense gradient of the species concentration and the gas temperature. Under such conditions the diffusion of different components of chemical reactions plays a significant role. It is particularly important for spray combustion where a two-stage ignition with cool- and hot-flame occurs. Thus a more complex model of multi-component diffusion was applied:

Maxwell-Stefan model for multi-component diffusion
$$\nabla X_i = \sum_{j \neq i} \frac{X_i X_j}{D_{ij}} \left(\mathbf{u}_{Dj} - \mathbf{u}_{Di} \right) \tag{8}$$

The diffusion rate $\boldsymbol{u}_{Di}$ is found by the method offered in [21]
$$\mathbf{u}_{Di} = -\frac{Dm_i}{X_i} \sum_j \nabla X_j \left(\delta_{ij} + A_{ij} + \sum_k A_{ik} A_{kj} \right) \tag{9}$$

$$A_{ij} = \delta_{ij} Y_i + X_i \frac{Dm_j}{D_{ij}} \left(1 - \delta_{ij} \right) \tag{10}$$

$$Dm_i = \frac{1 - Y_i}{\sum_{k \neq i} \frac{X_k}{D_{ik}}} \tag{11}$$

The properties of the gas mixture and of all components vary with temperature and pressure. The heat capacity $c_{pi}(T$ and the enthalpy $h_i(T)$ of each species, the binary diffusivity $D_{ij}(p,T)$ and the mixture´s thermal conductivity $\lambda(p,T)$ are calculated by the methods from [22].
The rate of chemical reactions was calculated by the equation:
$$\dot{w}_i = \mu_i \sum_{k_{reaction}} \left(\nu''_{i,k} - \nu'_{i,k} \right) A_k T^{n_k} e^{-\frac{E_k}{R^0 T}} \prod_{j_{species}} \left(\frac{X_j p}{R^0 T} \right)^{\nu'_{j,k}} \tag{12}$$

A complex reduced reaction mechanism for n-heptane with 62 steps (437 elementary reactions, 92 species in total, 25 steady-state species) was included in the numerical simulations. This reaction model was developed by the Institut für Technische Mechanik at RWTH Aachen. With the chemical kinetics, special attention was paid to the low- and high-temperature reactions. Details can be found in [23]. The reaction mechanism was optimized and validated by comparison with numerous experimental studies on droplet ignition in microgravity throughout the recent years [24-26].

Boundary Conditions

The center of the droplet ($r = 0$) is the point of symmetry where mass and energy fluxes are absent:
$$\mathbf{u}\big|_{r=0} = 0, \tag{13}$$

$$\left. \frac{\partial T}{\partial r} \right|_{r=0} = 0 \tag{14}$$

At the liquid-gas boundary ($r = r_s$), the conditions of mass and energy conservations are satisfied, as well as equality of temperature, and the conditions of gas-vapor equilibrium. That can be expressed by the following equations:

temperature equality
$$T_l \big|_{r=r_{s-}} = T_g \big|_{r=r_{s+}} \tag{15}$$

fugacity equilibrium $$f_i^l\Big|_{r=r_{s-}} = f_i^g\Big|_{r=r_{s+}}, \qquad f_i = X_i \cdot \phi_i \cdot p \tag{16}$$

mass conservation $$\rho_l\left(u_l - \dot{r}_s\right)\Big|_{r=r_{s-}} = \rho_g\left(u_g - \dot{r}_s\right)\Big|_{r=r_{s+}} = \dot{m} \tag{17}$$

species conservation $$Y_i^l \cdot \dot{m}\Big|_{r=r_{s-}} = Y_i\left(\dot{m} + \rho_g \cdot \mathbf{u}_{Di}\right)\Big|_{r=r_{s+}}, Y_i^l = \delta_{i,\,fuel} \tag{18}$$

energy conservation $$-\lambda_l \cdot \nabla T_l\Big|_{r=r_{s-}} + \dot{m} \cdot \Delta H_v = -\lambda_g \cdot \nabla T_g\Big|_{r=r_{s+}} \tag{19}$$

The fugacity coefficient ϕ_i is calculated by the method of Peng-Robinson [23]. The enthalpy of vaporization ΔH_v is expressed by the expression

$$\Delta H_v = \frac{\partial \ln\left(\phi_{fuel}^l \Big/ \phi_{fuel}^g\right)}{\partial\left(\frac{1}{T}\right)} R_{fuel} \tag{20}$$

Statements for the outer boundary ($r = r_{max}$) approximate the "spray" effects of the presence of neighboring droplets in the flow. The gas pressure in the calculation domain equals to the local pressure in the flow:

$$p = p_{out}(t) \tag{21}$$

For the reason of symmetry the mass and energy fluxes at the outer boundary ($r = r_{max}$) are absent:

$$\frac{\partial T}{\partial r}\Big|_{r=r_{\max}} = 0 \tag{22}$$

$$\mathbf{u}\big|_{r=r_{\max}} \approx \dot{r}_{\max} \tag{23}$$

The outer boundary is impenetrable for all species. In spite that a virtual source/sunk of air at the boundary of the numerical domain is included in order to approximate the jet mixing with the air flow:

$$j_{out} = \rho_{out} \cdot u_{out} \cdot r_{\max}^2 \tag{24}$$

where $$\rho_{out} = \rho_{air}\left(p, T_{out}\right)\big|_{r=r_{\max}} \tag{25}$$

$$j_{out} = -m_{fuel} \cdot \frac{1}{\varphi^2} \cdot \frac{d\varphi}{dt} \cdot \frac{1}{4\pi} \tag{26}$$

Therewith the fuel-air ratio φ within the numerical domain is equal to the local fuel-air ratio in the spray flow at each moment.

We have to note that such boundary conditions were only applied for simulations of JIC experiments in the HWT. For example, simulation of spray flows under conditions of diesel-engines need to take a higher spray density into account. In this case the energy flux seems to be more applicable like as

$$q_{out} = div\left(\lambda(T_{out} - T_{in})\right) \tag{27}$$

After its formation the droplets are strongly influenced by the incident flow up to moment when the droplets achieve the velocity of the main stream. A droplet´s shape is not spherical and the flow field around the droplet is perturbed by the main stream. Approximating a behavior at this stage the corrections of the gas diffusivity and the thermal conductivity were included in the numerical model. For this purpose Nusselt numbers for heat and mass transfer are applied.

$$\lambda_{gas}^{eff} = \lambda_{gas}^0 \cdot \frac{Nu}{Nu_0} \tag{28}$$

$$D_{m,i}^{eff} = D_{m,i}^0 \cdot \frac{Sh}{Sh_0} \tag{29}$$

Nusselt number *Nu* and Sherwood number *Sh* are expressed by:

$$Nu = 2 + 0.6 \cdot \sqrt{\mathrm{Re}} \cdot \sqrt[3]{\mathrm{Pr}} \tag{30}$$

$$Sh = 2 + 0.6 \cdot \sqrt{\mathrm{Re}} \cdot \sqrt[3]{Sc} \tag{31}$$

where *Re* is Reynolds number, *Pr* is Prandtl number, *Sc* is Schmidt number. $Nu_0 = 2$ and $Sh_0 = 2$ correspond to the values for an unperturbed flow field when the relative velocity of the droplet is zero. Though the Nusselt numbers are regarding steady-state and macroscopic scale, such approach gives good results: the evaporation time of droplets decreases essentially and approaches the values calculated with the CFD-code.

The proposed model was solved numerically using the finite-difference method. For this purpose a uniform mesh for the liquid phase and an exponential mesh for the gas phase were applied. Accounting for a stiff character of chemical kinetics equations the implicit backward differentiation method was applied by a manner of Winslow [24]. Changes of a step of time and an order of approximation are assumed. A data structure, methods of solution and successive approximations were optimized keeping an increase of a computing performance in mind. The code of the solver was implemented on the C++ programming language.

Results and Discussion

Figure 4 shows the results of a coupled spraylet simulation based on the experiment section of HWT. (Parameters are described above, see figure 2.) The droplet trajectories are shown during the time of 50 ms from the start of injection. From all packets only 100 droplet-tracks were chosen for the spraylet simulation. Initial droplet diameters, derived from the CFD-spray model, are between 20 and 70 µm. The gas temperature within the spraylet-domain is shown by color of the lines. The color of line turns into red when hot flame occurs. This is defined as a temperature gradient of 10^7 K/s.

Injected to a cross flow droplets form a non-uniform spatial distribution by affection through the incident flow and the different inertia of the droplets. Larger and heavier droplets move longer on the windward side of the spray core and penetrate the air flow deeper. On the contrary small droplets turn and evaporate faster and form a thin cloud on the leeward side of the spray. The same manner the earliest droplets injected to the main flow form the front of the spray and move under conditions which differ from those for the droplets following. Thus the start-time t_0 of a droplet can be introduced as the delay between this droplet´s injection and the moment when the first droplets were injected.

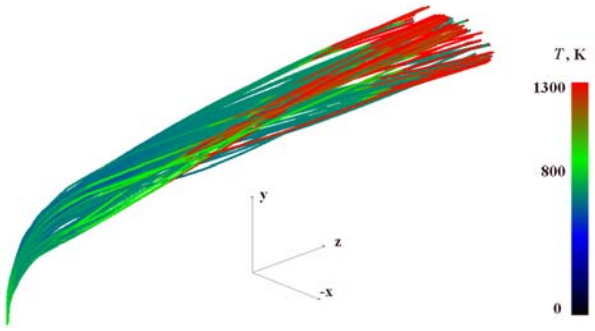

Figure 4 Spraylet trajectories with color changing into red where hot flame occurs

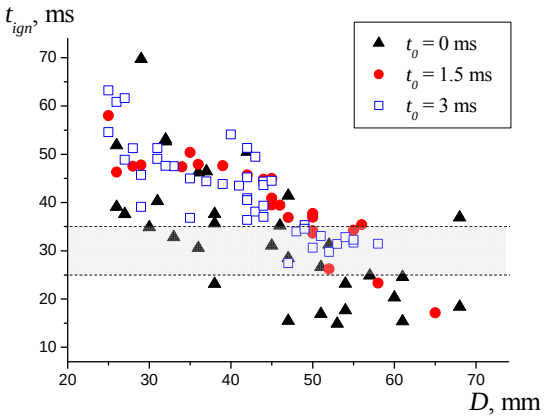

Figure 5 Total induction time of experiments (gray area) and numerical results (symbols) showing the effect of initial droplet size and the position in the spray (black triangles = front of the spray; red dots and blue squares = developed spray)

The effects of the initial droplet diameter D as well as of a droplet start-time t_0 are shown in Figure 5. In this figure the total induction times are presented for droplets of three start-times: 0 ms (front of the spray), 1.5 ms and 3 ms (middle section of the spray). As can be seen induction times are shorter for larger droplets in the spray as well as for the front of the spray. This can be explained by the position of heavier droplets on the windward side of the spray and by a higher gas temperature at this location. Also the shorter values and greater scattering for the induction time of droplets with the start-time $t_0 = 0$ (spray front) are noticeable.

The dispersion of experimental data of spray induction times is shown by the gray region between the dashed lines. Comparing the results, the following can be deduced: a) the effect of the spray front (triangles) seems to be overestimated by the simulation as no such soon ignition could be observed experimentally. b) The data of $t_0 = 1.5$ ms and $t_0 = 3$ ms mostly coincide. c) As expected, the droplets igniting the earliest seem to lead to the ignition of the ensemble in a whole. Thus a numerical prediction of the instant of spray ignition is on the safe side when reflecting onto the earliest igniting droplets. d) The droplets undergoing autoignition the earliest are of a diameter between 50 and 55 µm (with some very few exemptions). This coincides with the Mass-Median-Diameter (MMD) of the assumed spray which was exactly 53 µm.

Conclusion

The tasks-split spraylet approach enables the application of detailed droplet ignition simulations to large scale spray modeling. Inclusion of the micro scale and the chemically detailed models are the advantage for this approach. The numerical model of a coupling between single droplet simulations and a multidimensional spray flow simulation is presented. The complete spraylet simulation is realized for the example of a JIC spray. First results of the calculation show a good agreement with the experimental data. The detailed validation by comparison with experiments with parameters varied over a wider range is in progress.

Acknowledgements

Financial support through the German Aerospace Center, DLR, under grant 50 WM 0444 and 50 WM 0844 as well as through the European Space Agency, ESA, under grant AO-99-094 "CPS" is gratefully acknowledged.

References

[1] Aggarwal, S. K., 1998, *Progress in Energy and Combustion Science*, 24, pp. 565-600.

[2] Dhuchakallaya, I., Watkins, A.P., 2010, *Applied Energy*, 2010(87), pp. 1427–1432.

[3] Ge, H.-W., Gutheil, E., 2008, *Combustion and Flame*, 2008(153), pp. 173–185.

[4] Mastorakos, E., 2009, *Progress in Energy and Combustion Science*, 2009(35), pp. 57–97.

[5] Wang, Y., Rutland, C.J., 2004, *Proc. of the Combustion Institute*, T. C. Institute, ed., Elsevier, Chicago, pp. 893–900.

[6] Wang, Y., Rutland, C.J., 2007, *Combustion and Flame*, 2007(149), pp. 353–365.

[7] Williams, F. A., 2000, *Progress in Energy and Combustion Science*, 26, pp. 657-682.

[8] Novella, R., Garcia, A., Pastor, J.M., Domenech, V., 2011, *Math. and Comp. Modelling*, 54, pp. 1706-1719.

[9] Cuoci, A., Mehl, M., Buzzi-Ferraris, G., Faravelli, T., Manca, D., Ranzi, E., 2005, *Combustion and Flame*, 143(2005), pp. 211–226.

[10] Frolov, S. M., Basevich, V.Ya., Frolov, F.S., Borisov, A.A., Smetanjuk, V.A., Avdeev, K.A., Gots, A.N., 2009, *Russian J. of Phys. Chemistry, B*(3), pp. 333-347.

[11] Jin, Y., Shaw, B.D., 2010, *Int. J. Heat and Mass Transfer*, 53, pp. 5782-5791.

[12] Schnaubelt, S., Moriue, O., Eigenbrod, Ch. and Rath, H.J., 2001, *Microgravity, Science and Technology*, XIII(1), pp. 20-23.

[13] Schnaubelt, S., Eigenbrod, C., Rath, H.J., 2005, *Microgravity, Science and Technology*, 17(3), pp. 5-9.

[14] Stauch, R., Maas, U., 2007, *International Journal of Heat- and Mass Transfer*, 2007(50), pp. 3047–3053.

[15] Eigenbrod, C., Dittmer, Ch., Essmann, O., Rath, H.J., 2006, Drop Tower Days 2006 in Japan, *JASMA, Journal of The Japan Society of Microgravity Application*, Toki-Tsukuba, pp. 213-219.

[16] Rickmers, P., Eigenbrod, Ch., Klinkov, K., 2010, *IGTI Turbo-Expo 2010, Power for Land, Sea and Air*, ASME, ed.Glasgow.

[17] Dukowicz, J., 1980, *J. of Comp. Physics*, 35(2), pp. 229-253.

[18] Kuo, K. K., 2005, *Principles of Combustion*, Wiley.

[19] Williams, F. A., 1985, *Combustion Theory*, Addison Wesley.

[20] Reid, R. C., Prausnitz, J.M., Poling, B.E., 1988, *The properties of gases and liquids*, McGraw-Hill, New York.

[21] Oran, E. S., Boris, J.P., 1981, *Progress in Energy and Combustion Science*, 1981(7), pp. 1-72.

[22] Winslow, A. M., 1977, *J. Phys. Chem.*, 1977(81), pp. 2209-2413.

[23] Tanabe, M., Bolik, T., Eigenbrod, Ch., Rath, H.J., Sato, J., Kono. M., 1996, *26th Symposium (Int.) on Combustion*, T. C. Institute, ed., Elsevier, Naples, pp. 1637–1643.

[24] Eigenbrod, C., König, J., Moriue, O., Schnaubelt, S., Bolik, T., 1999, *Joint Meeting of the French, British and German Section of The Combustion Institute*, T. C. Institute, ed. Nancy, pp. 1-8.

[25] Schnaubelt, S., Moriue, O., Coordes, T., Eigenbrod, Ch. and Rath, H.J., 2000, *Proc. of the Combustion Institute*, T. C. Institute, ed., Elsevier, Edinburgh, pp. 953–960.

[26] Schnaubelt, S., Tanabe, O., Eigenbrod, C., Rath, H.J., 2000, *Space Forum*, 6(1-4(2000)), pp. 299-306.